



Published in final edited form as:

J Cyst Fibros. 2021 July ; 20(4): 664–672. doi:10.1016/j.jcf.2020.10.006.

DEFECTIVE IMMUNOMETABOLISM PATHWAYS IN CYSTIC FIBROSIS MACROPHAGES

Kaitlin Hamilton^a, Kathrin Krause^{a,1}, Asmaa Badr^a, Kylene Daily^a, Shady Estfanous^a, Mostafa Eltoigy^a, Arwa Abu Khweek^{a,e}, Midhun N.K. Anne^a, Cierra Carafice^a, Daniel Baetzhold^a, Jeffrey R. Tonniges^b, Xiaoli Zhang^c, Mikhail A. Gavrilin^d, Narasimham L. Parinandi^d, Amal O. Amer^a

^aDepartment of Microbial Infection and Immunity, College of Medicine, The Ohio State University, Columbus, OH 43210, USA

^bCampus Microscopy and Imaging Facility, The Ohio State University, Columbus, OH 43210, USA

^cCenter for Biostatistics, College of Medicine, The Ohio State University, Columbus, OH 43210, USA

^dDepartment of Internal Medicine, College of Medicine, The Ohio State University, Columbus, OH 43210, USA

^eDepartment of Biology and Biochemistry, Birzeit University, Birzeit, West Bank, Palestine

Abstract

Background: Mitochondria play a key role in immune defense pathways, particularly for macrophages. We and others have previously demonstrated that cystic fibrosis (CF) macrophages exhibit weak autophagy activity and exacerbated inflammatory responses. Previous studies have revealed that mitochondria are defective in CF epithelial cells, but to date, the connection between defective mitochondrial function and CF macrophage immune dysregulation has not been fully elucidated. Here, we present a characterization of mitochondrial dysfunction in CF macrophages.

Methods: Mitochondrial function in wild-type (WT) and CF F508del/F508del murine macrophages was measured using the Seahorse Extracellular Flux analyzer. Mitochondrial

Corresponding author: Dr. Amal O. Amer, Biomedical Research Tower, 460 W. 12th Avenue, Room 706, Columbus, OH 43210, USA; Amal.Amer@osumc.edu; Tel: (614) 247-1566; Fax: (614) 292-9616.

¹Present address: Max Planck Unit for the Science of Pathogens, Berlin, Germany

CRediT Author Statement:

Kaitlin Hamilton: Conceptualization, Methodology, Investigation, Formal Analysis, Writing —Original Draft, Writing — Review and Editing, Project Administration. **Kathrin Krause:** Methodology, Investigation, Writing — Review and Editing. **Asmaa Badr:** Investigation, Writing — Review and Editing. **Kylene Daily:** Investigation, Writing — Review and Editing. **Shady Estfanous:** Investigation, Writing — Review and Editing. **Mostafa Eltoigy:** Investigation, Writing — Review and Editing. **Arwa Abu Khweek:** Investigation, Writing — Review and Editing. **Midhun N.K. Anne:** Investigation, Writing — Review and Editing. **Cierra Carafice:** Investigation, Writing — Review and Editing. **Daniel Baetzhold:** Investigation, Writing — Review and Editing. **Jeffrey R. Tonniges:** Investigation, Writing — Review and Editing. **Xiaoli Zhang:** Formal analysis, Writing — Review and Editing. **Mikhail A. Gavrilin:** Investigation, Writing — Review and Editing. **Narasimham L. Parinandi:** Methodology, Investigation, Writing — Review and Editing. **Amal O. Amer:** Conceptualization, Methodology, Writing — Review and Editing, Supervision, Project Administration, Funding Acquisition.

Publisher's Disclaimer: This is a PDF file of an unedited manuscript that has been accepted for publication. As a service to our customers we are providing this early version of the manuscript. The manuscript will undergo copyediting, typesetting, and review of the resulting proof before it is published in its final form. Please note that during the production process errors may be discovered which could affect the content, and all legal disclaimers that apply to the journal pertain.

morphology was investigated using transmission electron and confocal microscopy. Mitochondrial membrane potential (MMP) as well as mitochondrial reactive oxygen species (mROS) were measured using TMRM and MitoSOX Red fluorescent dyes, respectively. All assays were performed at baseline and following infection by *Burkholderia cenocepacia*, a multi-drug resistant bacterium that causes detrimental infections in CF patients.

Results: We have identified impaired oxygen consumption in CF macrophages without and with *B. cenocepacia* infection. We also observed increased mitochondrial fragmentation in CF macrophages following infection. Lastly, we observed increased MMP and impaired mROS production in CF macrophages following infection with *B. cenocepacia*.

Conclusions: The mitochondrial defects identified are key components of the macrophage response to infection. Their presence suggests that mitochondrial dysfunction contributes to impaired bacterial killing in CF macrophages. Our current study will enhance our understanding of the pathobiology of CF and lead to the identification of novel mitochondrial therapeutic targets for CF.

Keywords

Mitochondria; macrophage; immunometabolism; reactive oxygen species; bacterial infection

1. Introduction

Dysfunctional macrophages are key contributors to the chronic infection and inflammation observed in cystic fibrosis (CF). Specifically, CF macrophages have defective autophagy, a cellular process that generates energy during stress or starvation but also removes pathogens[1,2]. We previously demonstrated that CF macrophages are permissive to *Burkholderia cenocepacia* (*B. cenocepacia*) infection due to impaired autophagy[1]. This bacterium infects 3–5% of CF patients and exhibits multi-drug resistance, association with a rapid decline in clinical course, and high mortality[3].

Mitochondria are key regulators of the macrophage infection response, an interaction termed “immunometabolism” [4]. When infected, healthy macrophages repurpose their mitochondria to increase mitochondrial reactive oxygen species (mROS) production while decreasing ATP production[5]. mROS promote pro-inflammatory macrophage activation and directly kill bacteria[4,6,7]. Reduced ATP production decreases the mitochondrial membrane potential (MMP) if left unchecked[8]. However, the MMP is sustained by the hydrolysis of glycolytic ATP[8]. Thus, reduced mitochondrial respiration is matched by increased glycolysis to provide ATP[4].

Mitochondrial abnormalities exist in CF epithelial cells, including impaired oxygen consumption, increased mROS, and oxidative stress[9–12]. However, the role of mitochondria in CF macrophage dysfunction has not been fully elucidated. One study identified altered mitochondrial oxygen consumption in human CF macrophages resulting from an upregulated unfolded protein response (UPR) pathway[13]. To fully understand the connection between mitochondrial and macrophage dysfunction in CF, it is critical to focus on the mitochondria and characterize their full set of defects in the absence and presence

of infection. This approach will provide the necessary groundwork to identify impaired immunometabolism pathways contributing to CF macrophage dysfunction.

Here, we report one such characterization using murine wild-type (WT) and CF F508del/F508del (CF) macrophages. We have identified several defects in CF mitochondria, including an impaired ability to respond to an increased energy demand at baseline and following *B. cenocepacia* infection and increased mitochondrial fragmentation and MMP along with impaired mROS production following infection. This suggests that mitochondrial dysfunction contributes to impaired bacterial killing in CF macrophages. Overall, our current study provides novel insights into the pathways contributing to CF macrophage dysfunction.

2. Methods

2.1. Ethics statement

Animal experiments were performed according to protocols approved by the Institutional Animal Care and Use Committee of The Ohio State University (Columbus, OH, USA).

2.2. Murine bone marrow-derived macrophages

WT C57BL/6J mice (JAX stock #000664) were purchased from The Jackson Laboratory (Bar Harbor, MD, USA). CF F508del/F508del mice on a C57BL/6J background (hereafter referred to as “CF”) were obtained from Case Western Reserve University’s CF Mouse Models Core (Cleveland, OH, USA). All mice were housed in a pathogen-free animal facility at The Ohio State University. Primary bone marrow-derived macrophages were generated and cultured as described[14].

2.3. Bacterial strains and culture

B. cenocepacia MH1K is a gentamicin-sensitive mutant of strain K56–2, a clinical isolate from a CF patient[15]. It was cultured as described[2]. MH1K was heat-inactivated at 60°C for 25 minutes.

Macrophages were infected at MOI 10 (live bacteria) or MOI 50 (heat-inactivated bacteria) for 1 h as described[14,16]. Following the infection, macrophages were treated with 50 ug/mL gentamicin for 0.5 h to inhibit extracellular bacterial replication. The addition of gentamicin was considered the 0 h time point.

2.4. Seahorse Extracellular Flux Analysis

Macrophages were seeded (70,000 cells/well) in a Seahorse 24-well plate (Agilent Technologies). Macrophages underwent a Cell Mito Stress Test in an XFe24 analyzer according to the manufacturer’s protocol. The XF assay media was supplemented with 10 mM glucose, 1 mM sodium pyruvate, and 2 mM L-glutamine. Electron transport chain (ETC) inhibitors were sequentially added to modulate oxygen consumption for mitochondrial function assessment: oligomycin (1 µM), FCCP (2 µM for non-infected, 1 µM for infected WT, and 1.5 µM for infected CF), and rotenone + antimycin A (0.5 µM). Inhibitor concentrations were optimized for each genotype and treatment condition. Results

were normalized to protein content measured using the Bradford method. Mitochondrial function parameters were calculated as described in the manufacturer's protocol.

2.5. Immunoblotting

Macrophages were lysed in TRIzol (ThermoFisher Scientific #15596018). Protein was extracted according to the manufacturer's protocol. Equal protein amounts were separated on a 15% or 13.5% SDS-PAGE gel and transferred to a PVDF membrane. Membranes were incubated overnight with the following antibodies: citrate synthase (1:1000, Cell Signaling Technologies #14309), Tom20 (1:1000, Sigma #WH0009804M1), cytochrome c (1:1000, Cell Signaling Technologies #11940), and GAPDH (1:1000, Cell Signaling Technologies #14C10). Protein bands were detected and analyzed as described[14].

2.6. Microscopy

For electron microscopy, macrophages were seeded on 2-well Permanox Lab-Tek chamber slides (Nunc 177429). Macrophages were fixed as described[1]. Sample processing and imaging was performed at the Campus Microscopy and Imaging Facility at The Ohio State University as described[1]. Mitochondrial morphology was manually quantified using ImageJ software (National Institutes of Health, Bethesda, MD) as described[17,18].

For fluorescence microscopy, macrophages were seeded on glass coverslips and stained with 250 nM MitoTracker Deep Red (Thermo Fisher Scientific M22426) for 15 minutes before infection. Macrophages were stained with 1 $\mu\text{g}/\text{mL}$ Hoechst 33342 (Thermo Fisher Scientific 62249) for 15 min before fixation with 4% paraformaldehyde for 0.5 h. Images were captured using an Olympus Fluoview FV10i laser scanning confocal microscope with a 60x objective. MitoTracker was pseudocolored in red.

2.7. TMRM assay

Macrophages were seeded (100,000 cells/well) in a black 96-well plate. Thirty minutes before the time point, macrophages were washed once in PBS and stained with 20 nM TMRM (Thermo Fisher Scientific T668) in imaging medium (10 mM HEPES, 1.8 mM CaCl_2 , 1 mM MgCl_2 , and 0.1% glucose in PBS). Fluorescence was measured on a SpectraMax i3x microplate reader at 548/574 nm and then normalized to cell number counted using a SpectraMax MiniMax 300 Imaging Cytometer.

2.8. ATP assay

Total ATP levels were measured using an ATP Detection Assay Kit (Cayman Chemical 700410). Macrophages were seeded (100,000 cells/well) in a 96-well plate. Macrophages were washed once in PBS and lysed in 1X Sample Buffer (200 $\mu\text{L}/\text{well}$). The lysates were diluted 1:10 in 1X Sample Buffer. The assay was performed according to the manufacturer's protocol. Luminescence was measured on a SpectraMax M5 microplate reader. An ATP standard curve was used to calculate ATP concentration, which was normalized to cell number as described in Section 2.7.

2.9. MitoSOX and DCFDA assays

Macrophages were seeded (100,000 cells/well) in a black 96-well plate and stained with 5 μ M MitoSOX Red (Thermo Fisher Scientific M36008) for 0.5 h or 10 μ M CM-H₂DCFDA (Thermo Fisher Scientific C6827) in imaging medium for 1 h before infection. This medium was used for the entire experiment to avoid fluorescence interference. Fluorescence was measured on a SpectraMax i3x microplate reader at 510/580 nm for MitoSOX and 485/515 nm for DCFDA and then normalized to cell number as described in Section 2.7.

2.10. Statistical analysis

Data were analyzed using SAS 9.4 (SAS Institute Inc., NC). All figures display mean and standard error of the mean (SEM) from at least three independent biological replicates or, for Fig. 3, 14–16 images from one biological replicate. Since independent biological replicates were analyzed, paired t-tests for two group comparisons or linear mixed effects models for multiple group comparisons were used to account for correlations among WT and CF observations from the same replicate. A two-way ANOVA was used for Fig. 3. P-values were adjusted with Holm's procedure for multiple comparisons. An adjusted p-value < 0.05 was considered statistically significant.

3. Results

3.1. CF macrophage mitochondria are less capable of responding to an increased energy demand at baseline and following *B. cenocepacia* infection

We began our mitochondrial function analysis using the Seahorse Analyzer, which monitors the oxygen consumption rate (OCR) in live cells (Fig. 1A–B). ETC inhibitors (oligomycin, FCCP, and rotenone + antimycin A) were sequentially added to modulate the OCR readings, which were then used to calculate several mitochondrial function parameters (Fig. 1C–E).

In non-infected macrophages, we observed no difference in basal respiration (BR) between WT and CF (Fig. 1C). BR represents respiration used to meet the endogenous ATP demand [19]. However, we observed significantly decreased maximal respiration (MR) and spare respiratory capacity (SRC) in CF versus WT macrophages (Fig. 1D–E). MR and SRC are both mitochondrial fitness indicators that represent how hard mitochondria can work when stressed and how capable they are at responding to an increased energy demand, respectively [19]. Thus, at baseline, CF macrophage mitochondria cannot work as hard as WT macrophage mitochondria and are less capable of increasing their function to meet an energy demand.

We next measured the OCR starting 5 h post-infection with *B. cenocepacia*. Both WT and CF macrophages significantly decreased their BR, MR, and SRC with infection (Fig. 1C–E). This reflects the mitochondrial repurposing that occurs following infection. However, infected CF macrophages had a significantly lower MR and SRC than infected WT macrophages (Fig. 1D–E). Together, these data reveal that CF macrophage mitochondria are less fit than WT macrophage mitochondria at baseline and that *B. cenocepacia* infection exacerbates this defect.

3.2. Decreased oxygen consumption in CF macrophages is not due to a difference in mitochondrial mass

Reduced OCR readings could be due to a defect in mitochondrial function or a decrease in mitochondrial mass. To distinguish between these possibilities, we examined mitochondrial mass via immunoblotting for three proteins from multiple mitochondrial compartments: Tom20, cytochrome c, and citrate synthase[20–22]. Monitoring multiple compartments is necessary because outer mitochondrial membrane proteins may be degraded independently of the rest of the mitochondrion[21,22]. We observed no significant differences in expression between WT and CF macrophages at baseline or following *B. cenocepacia* infection (Fig. 2). Therefore, the decreased OCR readings observed in CF macrophages are due to mitochondrial dysfunction and not a decrease in mitochondrial mass.

3.3. *B. cenocepacia* infection induces mitochondrial fragmentation in CF macrophages

Mitochondrial dysfunction is associated with changes in mitochondrial morphology[23]. We used transmission electron microscopy to examine three morphological parameters: area, elongation, and interconnectivity. Elongation represents mitochondrial shape with lower values signifying rounded, fragmented mitochondria[18]. Interconnectivity represents how connected the mitochondria are with lower scores signifying fragmentation[18]. At baseline, we observed no significant differences in WT and CF mitochondrial morphology (Fig. 3A–D). However, following 6 h of *B. cenocepacia* infection, CF mitochondria had significantly lower area, elongation, and interconnectivity scores compared to WT mitochondria (Fig. 3A–D). We were also able to observe these morphological changes using fluorescence microscopy. Following infection, WT mitochondria appeared in an interconnected, elongated network, while CF mitochondria appeared rounded and fragmented (Fig. 3E). This suggests that *B. cenocepacia* infection induces CF mitochondria fragmentation.

3.4. CF macrophage mitochondria have a higher mitochondrial membrane potential following *B. cenocepacia* infection

The metabolic shift from mitochondrial respiration to glycolysis with infection results in an increased MMP. We used TMRM, a fluorescent dye that accumulates in mitochondria as the MMP increases, to investigate this shift. At baseline, we observed no significant difference in MMP between WT and CF macrophages (Fig. 4A). Following *B. cenocepacia* infection, both WT and CF macrophages increased their MMP, a trend which reached significance at 8 h. This is indicative of the glycolytic shift. However, infected CF macrophages had a significantly higher MMP than infected WT macrophages at the 8 h time point (Fig. 4A). This suggests that CF macrophages are more glycolytic than WT macrophages following infection.

Next, we measured total ATP levels. Glycolysis is less efficient than mitochondrial respiration at producing ATP, so although glycolysis is upregulated, infected macrophages experience a decrease in total ATP levels[5]. We observed no difference in ATP levels between WT and CF macrophages at baseline or following 3 or 6 h of *B. cenocepacia* infection (Fig. 4B). Following 8 h of infection, both WT and CF macrophages significantly decreased their total ATP levels (Fig. 4B). This further demonstrates that infected WT and

CF macrophages have undergone the glycolytic shift. However, we observed no difference in total ATP levels between infected WT and CF macrophages.

3.5. CF macrophage mitochondria produce less mitochondrial ROS following *B. cenocepacia* infection

mROS play a key role in promoting inflammation and bacterial killing following infection. Elevated mROS levels were previously reported in CF epithelial cells[10,12,24]. We investigated whether mROS levels were also altered in CF macrophages using MitoSOX Red, a fluorescent dye that detects mitochondrial superoxide. At baseline, we observed no statistically significant difference in mROS between WT and CF macrophages (Fig. 5A). Following *B. cenocepacia* infection, both WT and CF macrophages similarly increased mROS over baseline levels (Fig. 5B).

Previously, we demonstrated that CF macrophages allow a significantly higher bacterial burden than WT macrophages due to defective autophagy[1,2]. It is possible that this higher bacterial burden masks an mROS production defect in CF macrophages. Therefore, we repeated the MitoSOX assay using heat-inactivated *B. cenocepacia* to ensure equal bacterial burdens between WT and CF macrophages. We verified that heat-inactivated *B. cenocepacia* do not replicate by preparing overnight cultures, which showed no growth (data not shown). Both WT and CF macrophages increased mROS over baseline levels following heat-killed *B. cenocepacia* infection (Fig. 5C). However, starting at 2 h post infection, CF macrophages began to slow down mROS production compared to WT macrophages, a trend which reached significance at 8 h (Fig. 5C). This reveals that a difference in bacterial burden is masking an mROS production defect. Overall, these results demonstrate that mROS production is impaired in infected CF macrophages.

For comparison, we measured ROS production in the whole cell using the fluorescent dye DCFDA. We observed no significant difference in cellular ROS production between WT and CF macrophages at baseline or following live or heat-killed *B. cenocepacia* infection (Fig. 5D–F).

4. Discussion

CF mitochondrial defects were identified in the 1970s, but with most research focused on the CFTR channel, there is still much we do not know about mitochondrial dysfunction in CF. The rapidly developing field of immunometabolism has highlighted the critical role that mitochondria play in governing macrophage function. We investigated this role in CF by characterizing mitochondrial defects in CF macrophages. Our study has revealed key defects in oxygen consumption, mitochondrial morphology, mROS production, and MMP in CF macrophage mitochondria at baseline and following *B. cenocepacia* infection. Since we utilized bone marrow-derived macrophages, these findings demonstrate that mitochondrial dysfunction is intrinsic to CF macrophages and exists prior to exposure to infection and the inflammatory lung environment.

Impaired mitochondrial oxygen consumption was previously identified in CF epithelial cells[9–11]. We also observed impaired oxygen consumption in CF macrophages, including

a significantly lower MR and SRC at baseline and following infection. This indicates that CF mitochondria are less capable of responding to an increased energy demand. However, a recent study observed the opposite effect following interferon- γ + lipopolysaccharide (LPS) stimulation where human CF macrophages had increased BR, MR, and SRC versus non-CF macrophages[13]. These data suggest that CF macrophages' metabolic response depends on the pro-inflammatory stimulus. This possibility is corroborated by a study in human monocytes that revealed stimuli-specific metabolic profiles for monocytes activated with LPS versus whole pathogen lysate[23].

Although we observed no difference in mitochondrial mass between WT and CF macrophages, we did observe increased fragmentation of CF mitochondria following *B. cenocepacia* infection. Modulating mitochondrial morphology is one way in which bacteria promote their survival during infections. *Legionella pneumophila*, for instance, directly interacts with macrophage mitochondria to induce fragmentation and damage, which promotes host cell glycolysis that supports efficient bacterial replication[25]. CF pathogens have been described exhibiting similar behaviors. *Pseudomonas (P.) aeruginosa* can promote mitochondrial fragmentation in epithelial cells[26]. Another study in epithelial cells found that *P. aeruginosa* uses succinate released by damaged mitochondria to drive airway colonization[27]. In macrophages, *Mycobacterium abscessus* was described interacting with mitochondria using glycopeptidolipids to regulate dissemination via apoptosis[28]. It is likely that *B. cenocepacia* also modulates mitochondrial morphology for its own benefit. The higher bacterial burden in CF macrophages may exacerbate this effect. Future studies will be needed to identify the mechanisms driving *B. cenocepacia*-induced mitochondrial fragmentation and how this contributes to its survival.

When responding to an infection, macrophages undergo a glycolytic shift to polarize into a pro-inflammatory M1 state[4]. Alternatively, macrophages can polarize into an anti-inflammatory M2 state[4]. It has been suggested that CF macrophages exhibit an M2 polarization defect[13]. Our data revealed that following *B. cenocepacia* infection, both WT and CF macrophages increased MMP and decreased total ATP levels, indicating a glycolytic shift. However, CF macrophages had a significantly higher MMP than WT macrophages, suggesting that infected CF macrophages are more glycolytic. Enhanced glycolysis in M1 macrophages combined with an M2 polarization defect may contribute to the exacerbated inflammatory responses observed in CF macrophages[1,29]. Identification of the individual contributions of glycolysis and mitochondrial respiration to the total ATP pool will be needed to confirm that infected CF macrophages are more glycolytic.

mROS serve a key role in the macrophage infection response by promoting inflammation and directly killing bacteria. Studies with CF epithelial cells revealed increased mROS production[10,12,24]. However, our study with CF macrophages revealed decreased mROS production following heat-killed *B. cenocepacia* infection. This suggests that cell type-specific alterations in mROS production exist in CF. It seems that CF epithelial cells overproduce mROS, but CF macrophages instead underproduce mROS.

Our finding of impaired mROS production in *B. cenocepacia*-infected CF macrophages has interesting implications regarding bacterial killing. Studies in healthy macrophages have

demonstrated that impairing mROS production results in defective bacterial killing[6,7]. Reduced mROS production may contribute to defective bacterial killing in CF macrophages in conjunction with impaired autophagy. Future work will be needed to investigate the role of mROS in bacterial killing in CF macrophages.

The link between CFTR dysfunction and mitochondrial dysfunction is currently unclear, but there are several hypotheses. One suggests that the chloride anion acts as a second messenger controlling the expression of genes regulating mitochondrial function[30]. Another suggests that accumulation of the misfolded CFTR protein upregulates the UPR pathway that then alters mitochondrial function[13]. What is clear is that mitochondrial dysfunction is an outcome of CF. Mitochondria play a critical role in the cell beyond producing ATP, especially in macrophages where they regulate the host infection response. Correcting mitochondrial defects may improve CF macrophage function. Future work building off of our current findings will help to identify mitochondria-based therapeutic targets that will contribute to resolving the chronic infection and inflammation characterizing CF.

Acknowledgements

We thank Dr. Miguel Valvano (Queen's University Belfast, UK) for kindly providing us with the *B. cenocepacia* MH1K stock. TEM images presented in this report were generated using the instruments and services at the Campus Microscopy and Imaging Facility, The Ohio State University. This facility is supported in part by grant P30 CA016058, National Cancer Institute, (Bethesda, MD, USA).

Funding:

Studies in the Amer laboratory are supported by the National Institute of Allergy and Infectious Diseases [R01 AI24121] and the National Heart, Lung, and Blood Institute [R01 HL127651-01A1]. The Amer laboratory is partially supported by a Research Development Program Grant (MCCOY19RO), "Cure Cystic Fibrosis Columbus (C3)", from the Cystic Fibrosis Foundation and the C3 Immune Core (C3IC). K.H. was supported by a Cure Cystic Fibrosis Columbus (Columbus, OH, USA) training grant and is now supported by a National Institutes of Health T32 training grant. K.K. was supported by a Cystic Fibrosis Foundation Post-doctoral research grant. A.B. and S.E. were supported by funding from the Egyptian Bureau of Higher Education. A.K. was supported by the Taawon Welfare Association (West Bank, Palestine) and the Bank of Palestine.

Declarations of interest

K.H. received training grants from Cure Cystic Fibrosis Columbus (Columbus, OH, USA) and the National Institutes of Health. K.K. received a grant from the Cystic Fibrosis Foundation. A.B. and S.E. received funding from the Egyptian Bureau of Higher Education. A.K. received funding from the Taawon Welfare Association and the Bank of Palestine. A.O.A. received grants from the National Institute of Allergy and Infectious Diseases, the National Heart, Lung, and Blood Institute, and Cure Cystic Fibrosis Columbus.

2Abbreviations:

CF	cystic fibrosis
WT	wild-type
MMP	mitochondrial membrane potential
mROS	mitochondrial reactive oxygen species production
UPR	unfolded protein response

OCR	oxygen consumption rate
ETC	electron transport chain
SEM	standard error of the mean
BR	basal respiration
MR	maximal respiration
SRC	spare respiratory capacity
NT	no treatment
HI	heat-inactivated
LPS	lipopolysaccharide

References:

- [1]. Abdulrahman BA, Khweek AA, Akhter A, Caution K, Kotrange S, Abdelaziz DHA, et al. Autophagy stimulation by rapamycin suppresses lung inflammation and infection by *Burkholderia cenocepacia* in a model of cystic fibrosis. *Autophagy*2011;7:1359–70. doi:10.4161/auto.7.11.17660. [PubMed: 21997369]
- [2]. Abdulrahman BA, Khweek AA, Akhter A, Caution K, Tazi M, Hassan H, et al. Depletion of the ubiquitin-binding adaptor molecule SQSTM1/P62 from macrophages harboring cftr f508 Mutation Improves the Delivery of *Burkholderia cenocepacia* to the Autophagic Machinery. *J Biol Chem*2013;288:2049–58. doi:10.1074/jbc.M112.411728. [PubMed: 23148214]
- [3]. Elborn JS, Balfour-Lynn IM, Bilton D. Respiratory disease: Infectious complications. In: Bush A, Hodson ME, Bilton D, editors. *Hodson Geddes' Cyst. Fibros.* 4th ed., CRC Press; 2015, p. 205–20.
- [4]. Mehta MM, Weinberg SE, Chandel NS. Mitochondrial control of immunity: beyond ATP. *Nat Rev Immunol*2017. doi:10.1038/nri.2017.66.
- [5]. Mills EL, Kelly B, Logan A, Costa ASH, Varma M, Bryant CE, et al. Succinate Dehydrogenase Supports Metabolic Repurposing of Mitochondria to Drive Inflammatory Macrophages. *Cell*2016;167:457–470.e13. doi:10.1016/j.cell.2016.08.064. [PubMed: 27667687]
- [6]. West AP, Brodsky IE, Rahner C, Woo DK, Erdjument-Bromage H, Tempst P, et al. TLR signalling augments macrophage bactericidal activity through mitochondrial ROS. *Nature*2011;472:476–80. doi:10.1038/nature09973. [PubMed: 21525932]
- [7]. Abuaita BH, Schultz TL, O'Riordan MX. Mitochondria-Derived Vesicles Deliver Antimicrobial Reactive Oxygen Species to Control Phagosome-Localized *Staphylococcus aureus*. *Cell Host Microbe*2018;24:625–636.e5. doi:10.1016/j.chom.2018.10.005. [PubMed: 30449314]
- [8]. EL Kasmi KC, Stenmark KR. Contribution of metabolic reprogramming to macrophage plasticity and function. *Semin Immunol*2015;27:267–75. doi:10.1016/j.smim.2015.09.001. [PubMed: 26454572]
- [9]. Valdivieso AG, Clauzure M, Marín MC, Taminelli GL, Massip Copiz MM, Sánchez F, et al. The Mitochondrial Complex I Activity Is Reduced in Cells with Impaired Cystic Fibrosis Transmembrane Conductance Regulator (CFTR) Function. *PLoS One*2012;7. doi:10.1371/journal.pone.0048059.
- [10]. Atlante A, Favia M, Bobba A, Guerra L, Casavola V, Reshkin SJ. Characterization of mitochondrial function in cells with impaired cystic fibrosis transmembrane conductance regulator (CFTR) function. *J Bioenerg Biomembr*2016;48:197–210. doi:10.1007/s10863-016-9663-y. [PubMed: 27146408]

- [11]. Kelly-Aubert M, Trudel S, Fritsch J, Nguyen-Khoa T, Baudouin-Legros M, Moriceau S, et al. GSH monoethyl ester rescues mitochondrial defects in cystic fibrosis models. *Hum Mol Genet* 2011;20:2745–59. doi:10.1093/hmg/ddr173. [PubMed: 21518732]
- [12]. Velsor LW, Kariya C, Kachadourian R, Day BJ. Mitochondrial oxidative stress in the lungs of cystic fibrosis transmembrane conductance regulator protein mutant mice. *Am J Respir Cell Mol Biol* 2006;35:579–86. doi:10.1165/rcmb.2005-0473OC. [PubMed: 16763223]
- [13]. Lara-Reyna S, Scambler T, Holbrook J, Wong C, Jarosz-Griffiths HH, Martinon F, et al. Metabolic Reprogramming of Cystic Fibrosis Macrophages via the IRE1a Arm of the Unfolded Protein Response Results in Exacerbated Inflammation. *Front Immunol* 2019;10:1789. doi:10.3389/fimmu.2019.01789. [PubMed: 31428093]
- [14]. Krause K, Caution K, Badr A, Hamilton K, Saleh A, Patel K, et al. CASP4/caspase-11 promotes autophagosome formation in response to bacterial infection. *Autophagy* 2018;14:1928–42. doi:10.1080/15548627.2018.1491494. [PubMed: 30165781]
- [15]. Hamad MA, Skeldon AM, Valvano MA. Construction of aminoglycoside-sensitive burkholderia cenocepacia strains for use in studies of intracellular bacteria with the gentamicin protection assay. *Appl Environ Microbiol* 2010;76:3170–6. doi:10.1128/AEM.03024-09. [PubMed: 20348312]
- [16]. Zhang S, Shrestha CL, Kopp BT. Cystic fibrosis transmembrane conductance regulator (CFTR) modulators have differential effects on cystic fibrosis macrophage function. *Sci Rep* 2018;8:1–10. doi:10.1038/s41598-018-35151-7. [PubMed: 29311619]
- [17]. Dagda RK, Cherra SJ, Kulich SM, Tandon A, Park D, Chu CT. Loss of PINK1 function promotes mitophagy through effects on oxidative stress and mitochondrial fission. *J Biol Chem* 2009;284:13843–55. doi:10.1074/jbc.M808515200. [PubMed: 19279012]
- [18]. Wiemerslage L, Lee D. Quantification of mitochondrial morphology in neurites of dopaminergic neurons using multiple parameters. *J Neurosci Methods* 2016;262:56–65. doi:10.1016/j.jneumeth.2016.01.008. [PubMed: 26777473]
- [19]. Divakaruni AS, Paradyse A, Ferrick DA, Murphy AN, Jastroch M. Analysis and interpretation of microplate-based oxygen consumption and pH data. In: Murphy AN, Chan DC, editors. *Methods Enzymol*, vol. 547, Elsevier Inc.; 2014, p. 309–54. doi:10.1016/B978-0-12-801415-8.00016-3. [PubMed: 25416364]
- [20]. Redmann M, Benavides GA, Berryhill TF, Wani WY, Ouyang X, Johnson MS, et al. Inhibition of autophagy with bafilomycin and chloroquine decreases mitochondrial quality and bioenergetic function in primary neurons. *Redox Biol* 2017;11:73–81. doi:10.1016/j.redox.2016.11.004. [PubMed: 27889640]
- [21]. Chan NC, Salazar AM, Pham AH, Sweredoski MJ, Kolawa NJ, Graham RLJ, et al. Broad activation of the ubiquitin-proteasome system by Parkin is critical for mitophagy. *Hum Mol Genet* 2011;20:1726–37. doi:10.1093/hmg/ddr048. [PubMed: 21296869]
- [22]. Ding WX, Yin XM. Mitophagy: Mechanisms, pathophysiological roles, and analysis. *Biol Chem* 2012;393:547–64. doi:10.1515/hsz-2012-0119. [PubMed: 22944659]
- [23]. Lachmandas E, Boutens L, Ratter JM, Hijmans A, Hooiveld GJ, Joosten LAB, et al. Microbial stimulation of different Toll-like receptor signalling pathways induces diverse metabolic programmes in human monocytes. *Nat Microbiol* 2016;2. doi:10.1038/nmicrobiol.2016.246.
- [24]. Clazure M, Valdivieso AG, Massip Copiz MM, Schulman G, Teiber ML, Santa-Coloma TA. Disruption of interleukin-1 β autocrine signaling rescues complex I activity and improves ROS levels in immortalized epithelial cells with impaired Cystic Fibrosis Transmembrane Conductance Regulator (CFTR) function. *PLoS One* 2014;9:1–17. doi:10.1371/journal.pone.0099257.
- [25]. Escoll P, Song OR, Viana F, Steiner B, Lagache T, Olivo-Marin JC, et al. Legionella pneumophila Modulates Mitochondrial Dynamics to Trigger Metabolic Repurposing of Infected Macrophages. *Cell Host Microbe* 2017;22:302–316.e7. doi:10.1016/j.chom.2017.07.020. [PubMed: 28867389]
- [26]. Maurice NM, Bedi B, Yuan Z, Goldberg JB, Koval M, Hart CM, et al. Pseudomonas aeruginosa Induced Host Epithelial Cell Mitochondrial Dysfunction. *Sci Rep* 2019;9:11929. doi:10.1038/s41598-019-47457-1. [PubMed: 31417101]

- [27]. Riquelme SA, Lozano C, Moustafa AM, Liimatta K, Tomlinson KL, Britto C, et al. CFTR-PTEN-dependent mitochondrial metabolic dysfunction promotes *Pseudomonas aeruginosa* airway infection. *Sci Transl Med* 2019;11:eaav4634. doi:10.1126/scitranslmed.aav4634. [PubMed: 31270271]
- [28]. Whang J, Back YW, Lee KI, Fujiwara N, Paik S, Choi CH, et al. Mycobacterium abscessus glycopeptidolipids inhibit macrophage apoptosis and bacterial spreading by targeting mitochondrial cyclophilin D. *Cell Death Dis* 2017;8:e3012. doi:10.1038/cddis.2017.420. [PubMed: 28837151]
- [29]. Kopp BT, Abdulrahman BA, Khweek AA, Kumar SB, Akhter A, Montione R, et al. Exaggerated inflammatory responses mediated by *Burkholderia cenocepacia* in human macrophages derived from cystic fibrosis. *Biochem Biophys Res Commun* 2012;424:221–7. doi:10.1016/j.bbrc.2012.06.066.EXAGGERATED. [PubMed: 22728038]
- [30]. Valdivieso ÁG, Clazure M, Massip-Copiz M, Santa-Coloma TA. The Chloride Anion Acts as a Second Messenger in Mammalian Cells - Modifying the Expression of Specific Genes. *Cell Physiol Biochem* 2016;38:49–64. doi:10.1159/000438608. [PubMed: 26741366]

Highlights

Mitochondria in CF macrophages are less capable of responding to energetic stress.

B. cenocepacia infection further exacerbates this mitochondrial defect.

CF mitochondria have a higher membrane potential following infection.

CF macrophages produce less mitochondrial ROS following infection.

Mitochondrial defects can impair bacterial killing and augment inflammation.

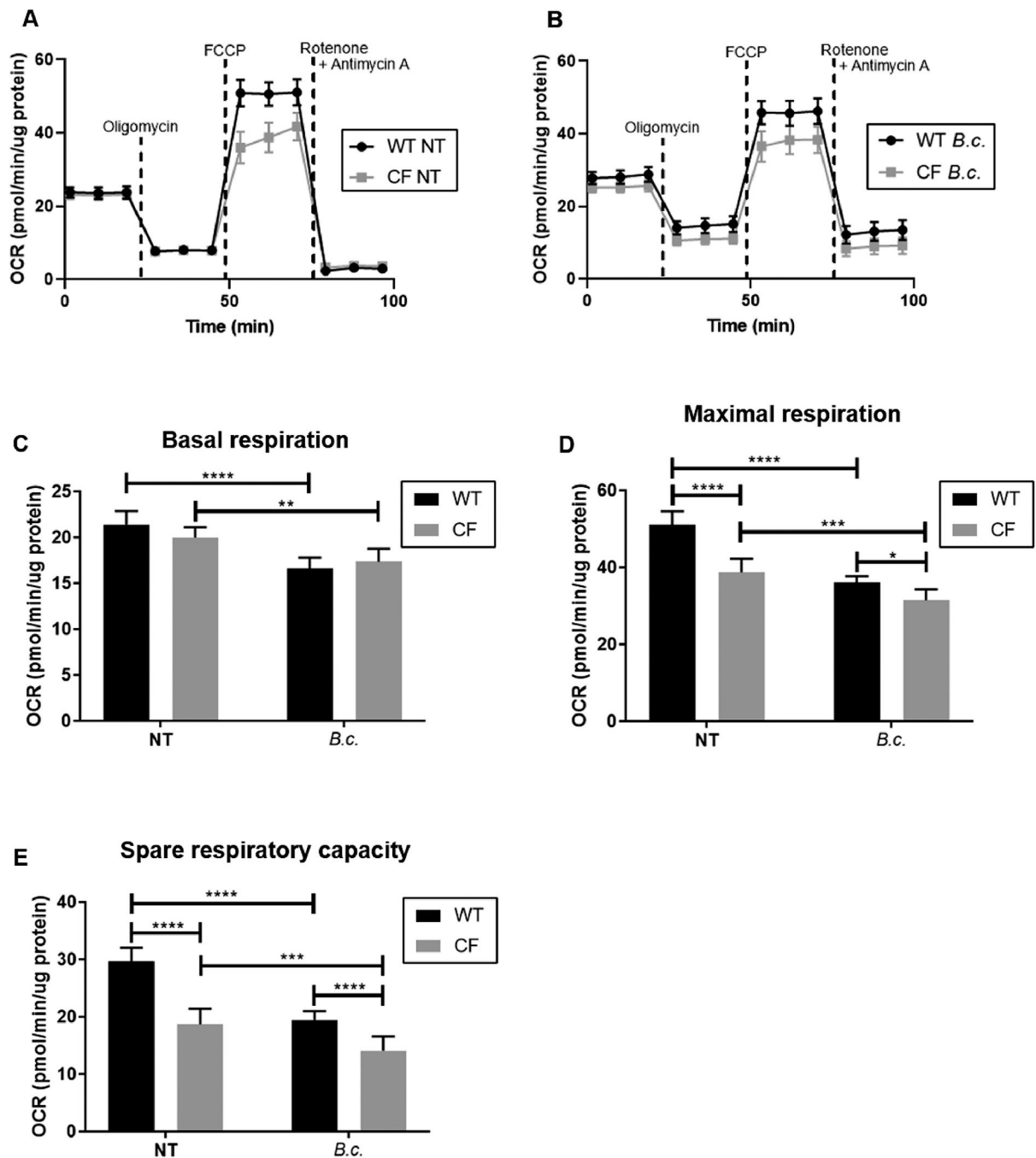


Fig. 1: Mitochondria in CF macrophages are less capable of responding to an increased energy demand at baseline and following *B. cenocepacia* infection

Seahorse Cell Mito Stress Test performed in WT and CF macrophages at baseline (NT = no treatment) or following 5 h *B. cenocepacia* (*B.c.*) infection. (A-B) Oxygen consumption rate (OCR) was measured following the addition of ETC inhibitors to investigate mitochondrial function. (C-E) Mitochondrial function parameters calculated from (A-B). Graphs show mean and SEM. N=7 WT and CF mice. Statistics: Linear mixed effects model with Holm's post-test. *, $p < 0.05$; **, $p < 0.01$; ***, $p < 0.001$; ****, $p < 0.0001$.

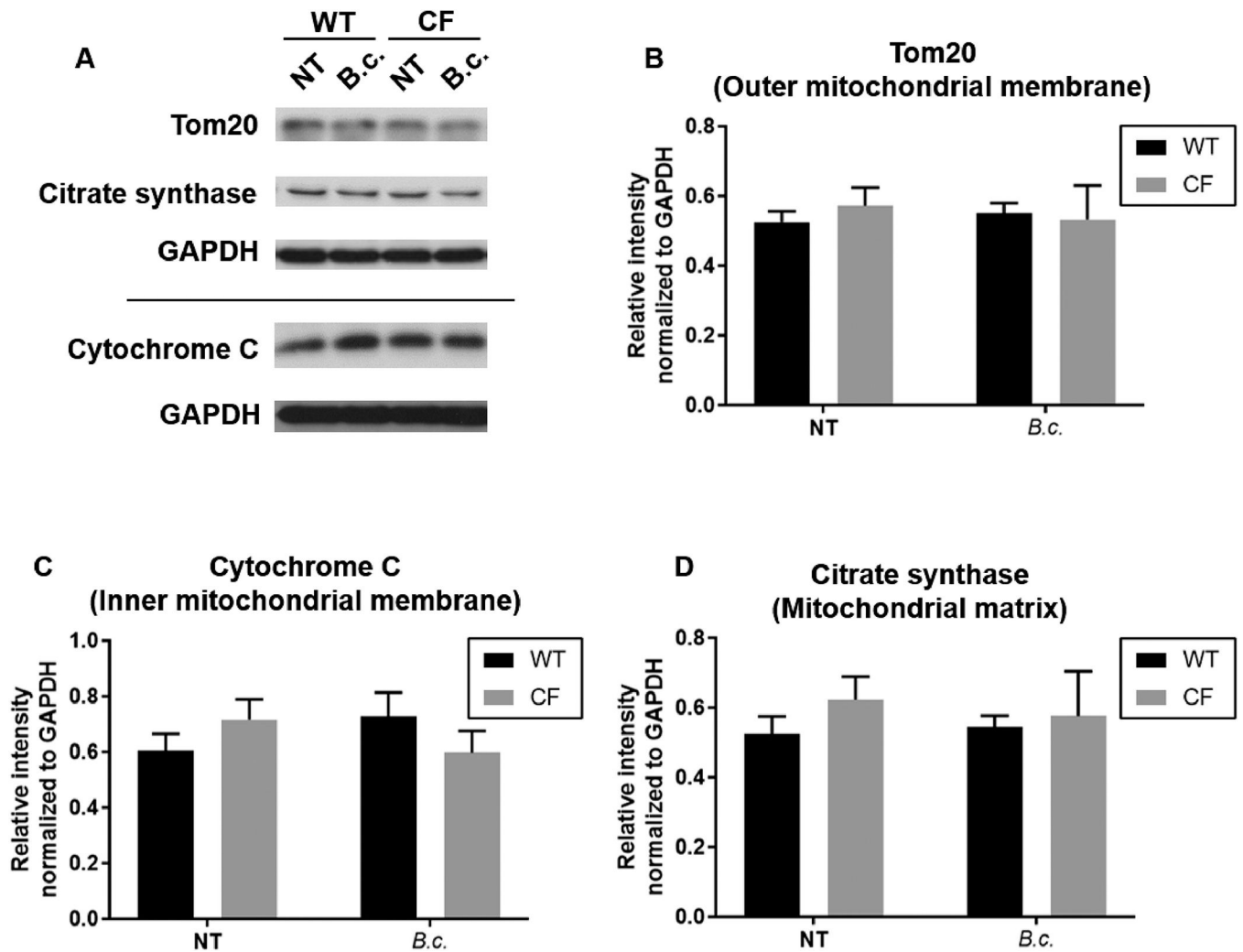


Fig. 2: Decreased oxygen consumption in CF macrophages is not due to a difference in mitochondrial mass

Immunoblot for mitochondrial proteins in WT and CF macrophages at baseline (NT) and following 6 h *B. cenocepacia* (*B.c.*) infection. (A) Representative immunoblots. (B-D) Densitometry analysis. Graphs show mean and SEM. N=5 WT and CF mice. Statistics: Linear mixed effects model with Holm's post-test.

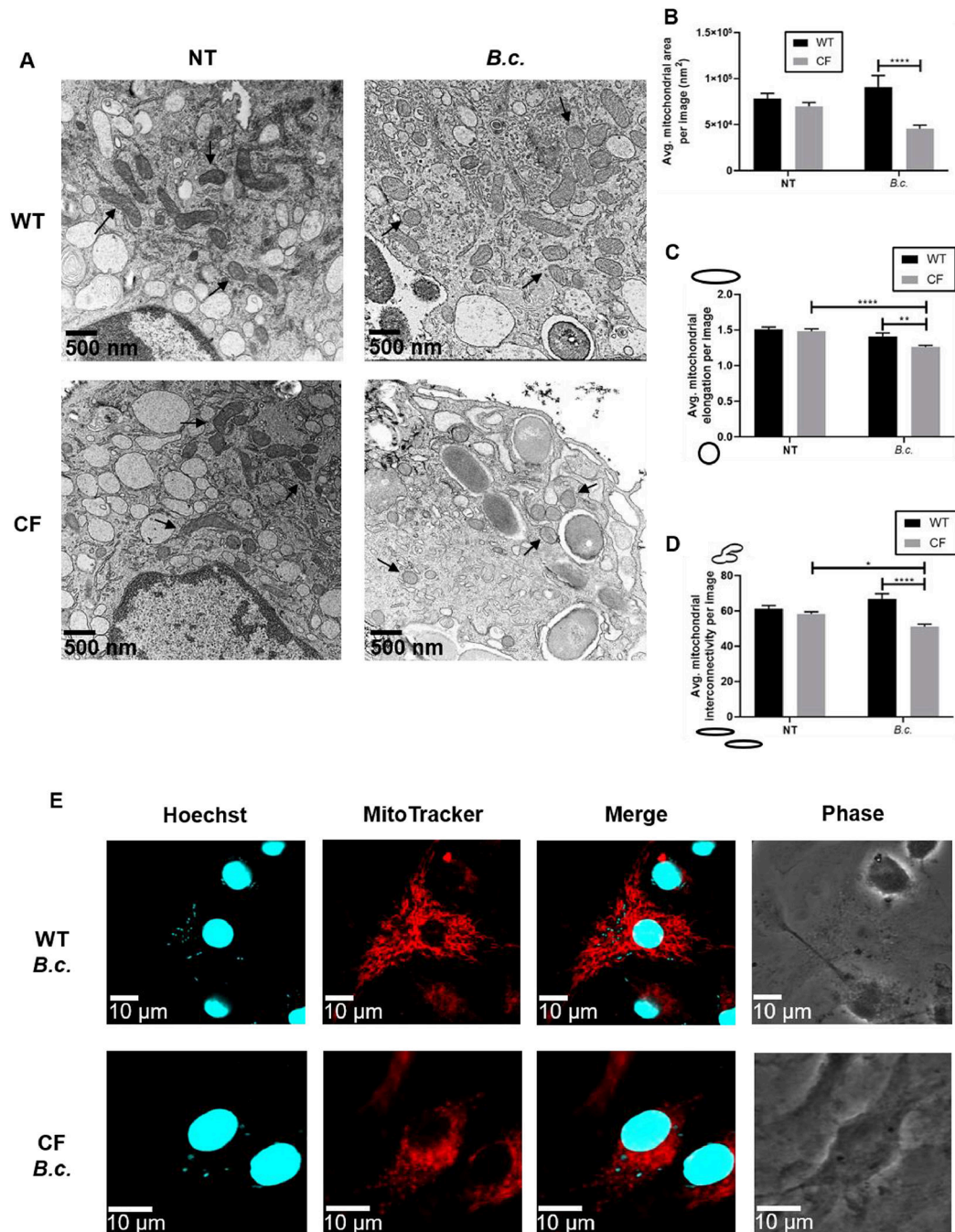


Fig. 3: *B. cenocepacia* infection induces mitochondrial fragmentation in CF macrophages
 Microscopy analysis of mitochondrial morphology in WT and CF macrophages at baseline (NT) and following 6 h *B. cenocepacia* (*B.c.*) infection. (A) Representative electron microscopy images taken at 22,500x magnification. Several mitochondria are indicated with arrows. (B-D) Mitochondrial morphology parameters calculated from electron microscopy images. Parameters were calculated for individual mitochondria then averaged per image. For the elongation and interconnectivity graphs, sketches next to the y-axis indicate the morphology represented by low vs. high scores. Graphs show mean and SEM. N=1 WT

and CF mouse; 14–16 images analyzed per condition. Statistics: Two-way ANOVA with Holm's post-test. *, $p < 0.05$; **, $p < 0.01$; ***, $p < 0.001$; ****, $p < 0.0001$. (E) Representative fluorescence microscopy images. MitoTracker Deep Red was used to stain the mitochondria. Hoechst 33342 was used to stain the macrophage nuclei and *B. cenocepacia*.

Author Manuscript

Author Manuscript

Author Manuscript

Author Manuscript

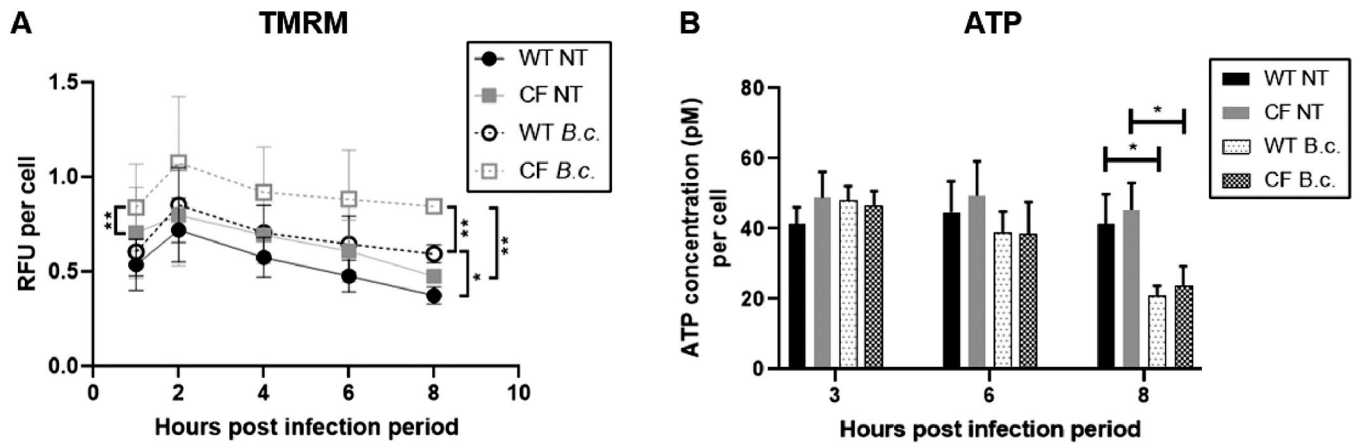


Fig. 4: Mitochondria in CF macrophages have a higher mitochondrial membrane potential following *B. cenocepacia* infection

TMRM (A) and ATP (B) assays performed in WT and CF macrophages at baseline (NT) and following *B. cenocepacia* (*B.c.*) infection. RFU = Relative fluorescence units. Graphs show mean and SEM. N=3 WT and CF mice for (A) and N=4 WT and CF mice for (B). Statistics: Linear mixed effects model with Holm's post-test for each time point. *, $p < 0.05$; **, $p < 0.01$.

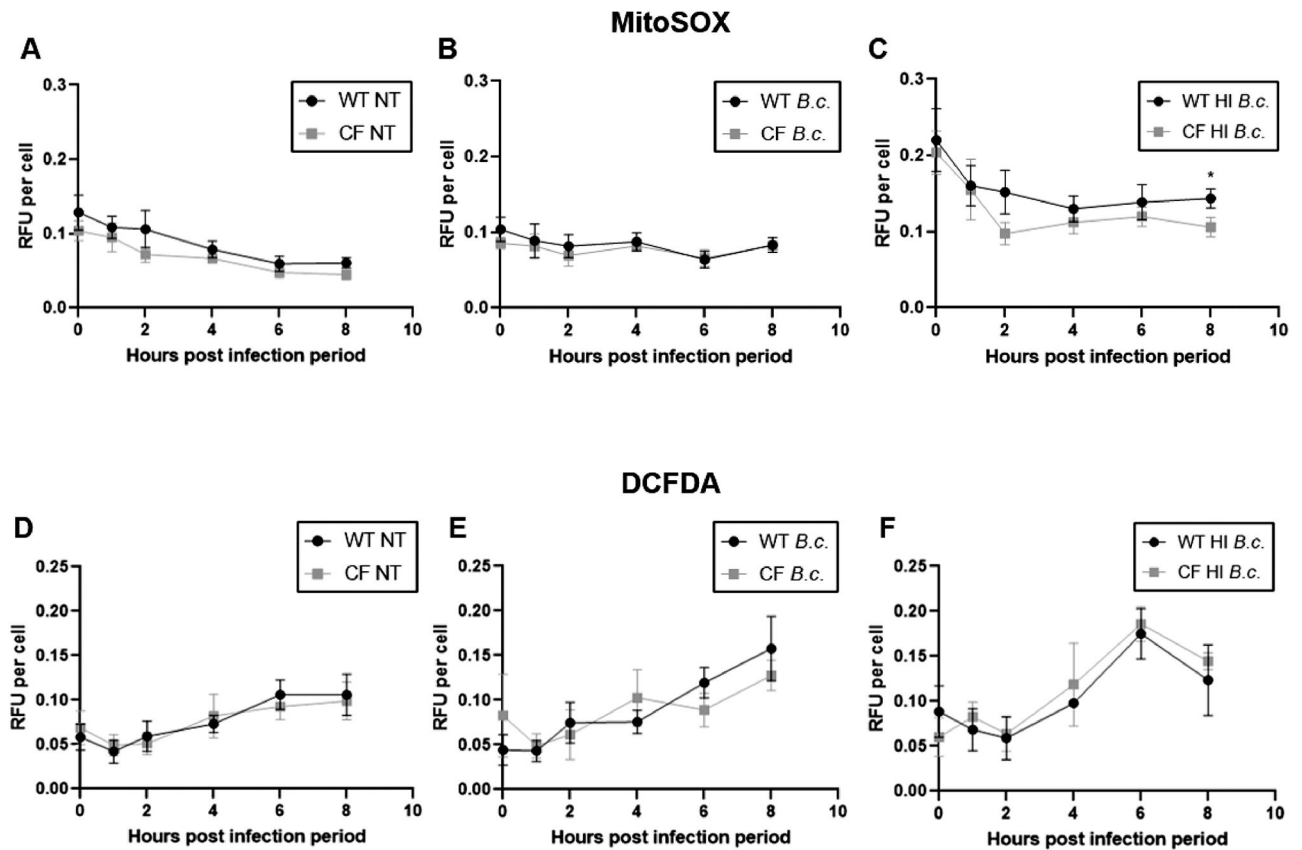


Fig. 5: Mitochondria in CF macrophages produce less mitochondrial ROS following *B. cenocepacia* infection

MitoSOX (A-C) and DCFDA (D-E) assays performed in WT and CF macrophages at baseline (NT) and following infection with live or heat-inactivated (HI) *B. cenocepacia* (*B.c.*). Graphs show mean and SEM. N=10–14 WT and CF mice for (A), N=5–7 WT and CF mice for (B), N=5–7 WT and CF mice for (C), N=8–10 WT and CF mice for (D), N=5–7 WT and CF mice for (E), and N=3 WT and CF mice for (F). Statistics: Two-tailed paired t-test for each time point. *, $p < 0.05$.